J Mater Sci (2022) 57:6971–6987

Computation & theory

Theoretical insights into the nonlinear optical properties of cyclotriphosphazene ($P_3N_3Cl_6$), tris(4–hydroxyphenyl) ethane and their various inorganic–organic hybrid derivatives

Majid Basharat[1,2] and Djebar Hadji[3,4,*]

[1] Institute for Advanced Study, Shenzhen University, Nanhai Avenue 3688, Shenzhen 518060, People's Republic of China
[2] College of Physics and Optoelectronic Engineering, Shenzhen University, 518060 Shenzhen, People's Republic of China
[3] Department of Chemistry, Faculty of Sciences, University of Saida – Dr. Moulay Tahar, 20000 Saida, Algeria
[4] Modeling and Calculation Methods Laboratory, University of Saida – Dr. Moulay Tahar, 20000 Saida, Algeria

Received: 10 November 2021
Accepted: 7 March 2022
Published online: 25 March 2022

ABSTRACT

With the rapid developments of computational methods, now it is effective and efficient to predict properties and underlying reasons at different stages. In this work, we systematically investigated hexachlorocyclotriphosphazene, tris(4–hydroxyphenyl) ethane and their various inorganic–organic hybrid derivatives for dipole moment, polarizability and static first hyperpolarizability. The relation between the nonlinear optical (NLO) properties and the energy gaps were also considered. The geometries of these inorganic–organic hybrid derivatives at different substitution positions have been performed using the B3LYP functional. The ωB97X–D and B3LYP functionals give the high static first hyperpolarizability compared to the CAM–B3LYP and M05–2X levels. Inverse relation has been obtained between the HOMO–LUMO gaps and the hyper-Rayleigh scattering (HRS) first hyperpolarizability β_{HRS}. This theoretical study reveals underlying changes in the design structures, and shift in properties will provide better understanding and may grab the attention of researchers to study cross-linkable organocyclotriphosphazenes for NLO application.

Handling Editor: Andrea de Camargo.

Address correspondence to E-mail: hadji120780@yahoo.fr; djebar.hadji@univ–saida.dz

https://doi.org/10.1007/s10853-022-07088-w

GRAPHICAL ABSTRACT

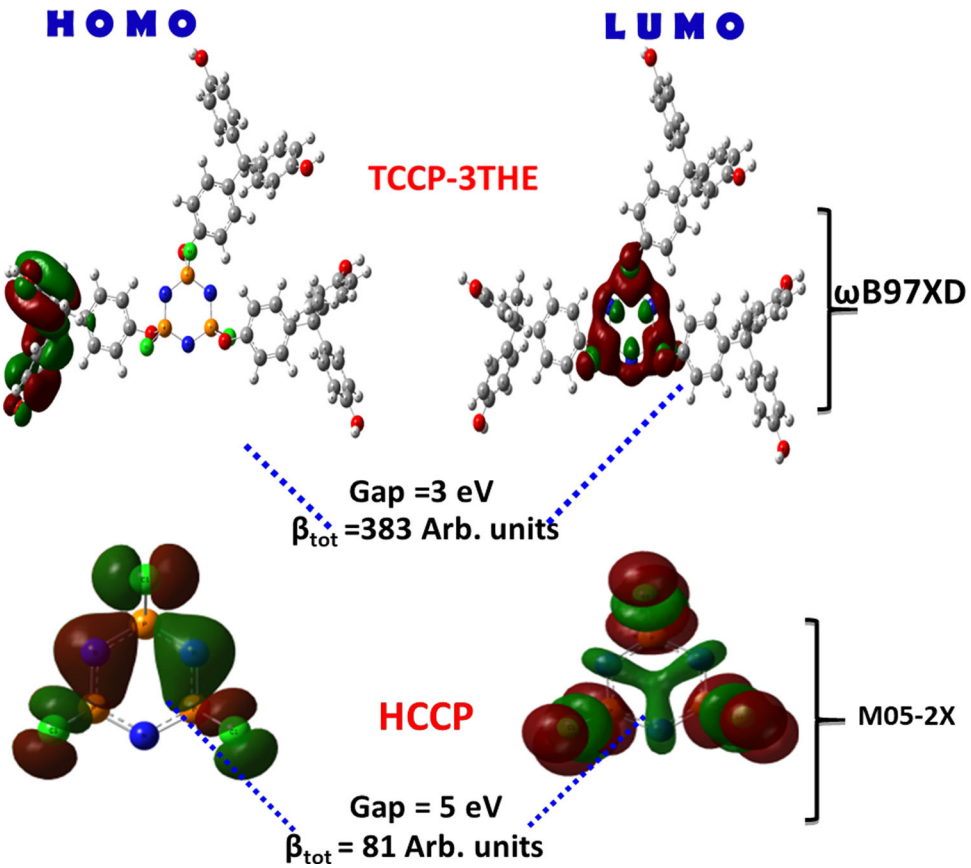

Introduction

The properties at the molecular or microscopic level of materials allow the description of their properties at the macroscopic level. Understanding the mechanisms that govern its properties and their expressions at the macroscopic level from molecular properties is an important requirement when developing devices with a desired property. With rapid developments of first-principles methods in studying materials, now it is effective and efficient to predict without any experimental data at different stages. The compounds incorporating a phosphazene bond (–P = N–) are interchangeably called phosphinimines, phosphazenes, or iminophosphoranes. Under these different names are grouped different families of molecules incorporating the P = N bond, opening a wide field in the chemistry of phosphorus compounds. Many organophosphorus polymers have been studied [1–3], which are able to bind with metal surfaces [4–6], and for biological applications [7]. Their clinical utility against microbial activity gives them an increasing interest. Also, the broad range of properties they exhibit and the attached group to the phosphorus [8], make the phosphazene materials very interesting. This material type has low glass-transition temperatures, is resistant to degradation by hydrocarbons and can be used as arctic fuel lines [9]. Also, this material may have applications such as solid-state batteries [10]. Several theoretical and experimental papers [11–14] show the suitability of phosphazenes in NLO field. The phosphazene compounds like spirocyclophosphazenes studied by Maturana et al. [12] have charge transfer which mainly depends on the electron delocalization. We note that the cyclotriphosphazenes can

act as host specie in the host–guest interaction system [15–17]. The cyclotriphosphazenes can use in polymer [16] and be used to obtain systems with transition metal [18]. The presence of the cyclotriphosphazene in the design of materials was expected to increase the flame resistance and the thermal stability in polyphosphazenes [19–22] such as the hexakis(4–aminophenoxy)cyclotriphosphazene-based polyimide matrices [22]. Cyclotriphosphazenes belong to a growing family of channel-type inclusion compounds [23, 24]. Indeed, the tris(o–phenylenedioxy)cyclotriphosphazene can act as channel in supramolecular-wire confinement of I_2. Nevertheless, the most important works, which interest us, have concerned the chlorocyclotriphosphazene group participation to increase the NLO properties in materials [25–27]. Following Kang et al. [28], the large polarizability anisotropy $\Delta\alpha$ and the first-order hyperpolarizability β of our organocyclo–phosphazenes can reflect the macroscopic birefringence and SHG like phosphazenes with skeletal architectures –P = N–P = N–P = N–, and like cyano-based materials. The recent works of phosphazene [12, 13, 29, 30] showed the suitability of phosphazenes and organophosphazenes for the NLO applications. In this study, we investigated the inorganic ring hexachlorocyclotriphosphazene (HCCP), organic comonomer tris(4–hydroxyphenyl) ethane (THE), and their derived core organo–cyclotriphosphazene structure series where the cyclotriphosphazene ring substituted with THE at different positions [31]. These compounds are noted (Fig. 1): HCCP (hexachlorocyclotriphosphazene), THE (tris(4–hydroxyphenyl) ethane), PCCP–THE (pentachclorocyclotriphosphazene–co–tris(4–hydroxyphenyl) ethane)), TCCP–gem2THE (tetrachclorocyclotriphosphazene–co–gem2(tris(4–hydroxyphenyl) ethane, TCCP–2THE (tetrachclorocyclotriphosphazene–co–2(tris(4–hydroxyphenyl) ethane), TCCP–3THE: trichlorocyclotriphosphazene–co–3(tris(4–hydroxyphenyl) ethane), DCCP–4THE (dichlorocyclotriphosphazene–co–4(tris(4–hydroxyphenyl) ethane)), 3PCCP–THE 3(pentachclorocyclotriphosphazene)–co–tris(4–hydroxyphenyl) ethane.

Methods

Computational chemistry methods are used to predict the linear and NLO properties of organocyclo–phosphazenes. The study reveals that cyclotriphosphazene compounds linked to tris(4–hydroxyphenyl) ethane groups are a remarkably large first-order NLO response. The results obtained from the density functional theory (DFT) will provide the electronic properties of this important class of phosphazenes. At first time, the geometry optimizations for all organocyclophosphazenes are performed within DFT method at the B3LYP functional using the 6–311 + G(d) basis set. No constraints on geometries were implemented. Real values for all vibrational frequencies confirmed that the optimized geometries of the studied phosphazenes correspond to minima on the potential energy surface. All linear (dipole moment μ, mean polarizability $\langle\alpha\rangle$, and anisotropy polarizability $\Delta\alpha$) and NLO properties (gas phase electric field-induced second harmonic generation (EFISHG) $\beta_{//}(-2\omega;\omega,\omega)$, the hyper–Rayleigh scattering (HRS) first hyperpolarizability β_{HRS} (− 2ω; ω, ω), and the depolarization ratios (DR)) are calculated in the gas phase at different DFT levels (B3LYP, ωB97X–D, CAM–B3LYP, and M05–2X functionals [32–37]) in association with the 6–311 + G(d) and aug–cc–pVDZ basis sets. The efficiency of range separated and DFT hybrid functionals in polarizability and first hyperpolarizability calculations is studied less extensively. Hyperpolarizabilities considerable improvements were reported when the fraction of Hartree–Fock exchange in the hybrid functional increased up to 56% [38–40]. In Fig. 2, we present the optimized geometries of the cyclophosphazene and their derived organocyclo–phosphazenes at the B3LYP/6–311 + G(d) level.

The total dipole moment was defined as follows:

$$\mu = \sqrt{\left(\mu_x^2 + \mu_y^2 + \mu_z^2\right)} \tag{1}$$

Using the polarizability components obtained by the Gaussian out file, the average polarizability $\langle\alpha\rangle$ was calculated using the polarizability components by the formula

$$\langle\alpha\rangle = \frac{1}{3}\sum_{i=x,y,z}\alpha_{ii} \tag{2}$$

and the $\Delta\alpha$ as:

$$\Delta\alpha = \sqrt{\frac{1}{2}\left[\left(\left(\alpha_{xx}-\alpha_{yy}\right)^2 + \left(\alpha_{xx}-\alpha_{zz}\right)^2 + \left(\alpha_{yy}-\alpha_{zz}\right)^2\right)\right]} \tag{3}$$

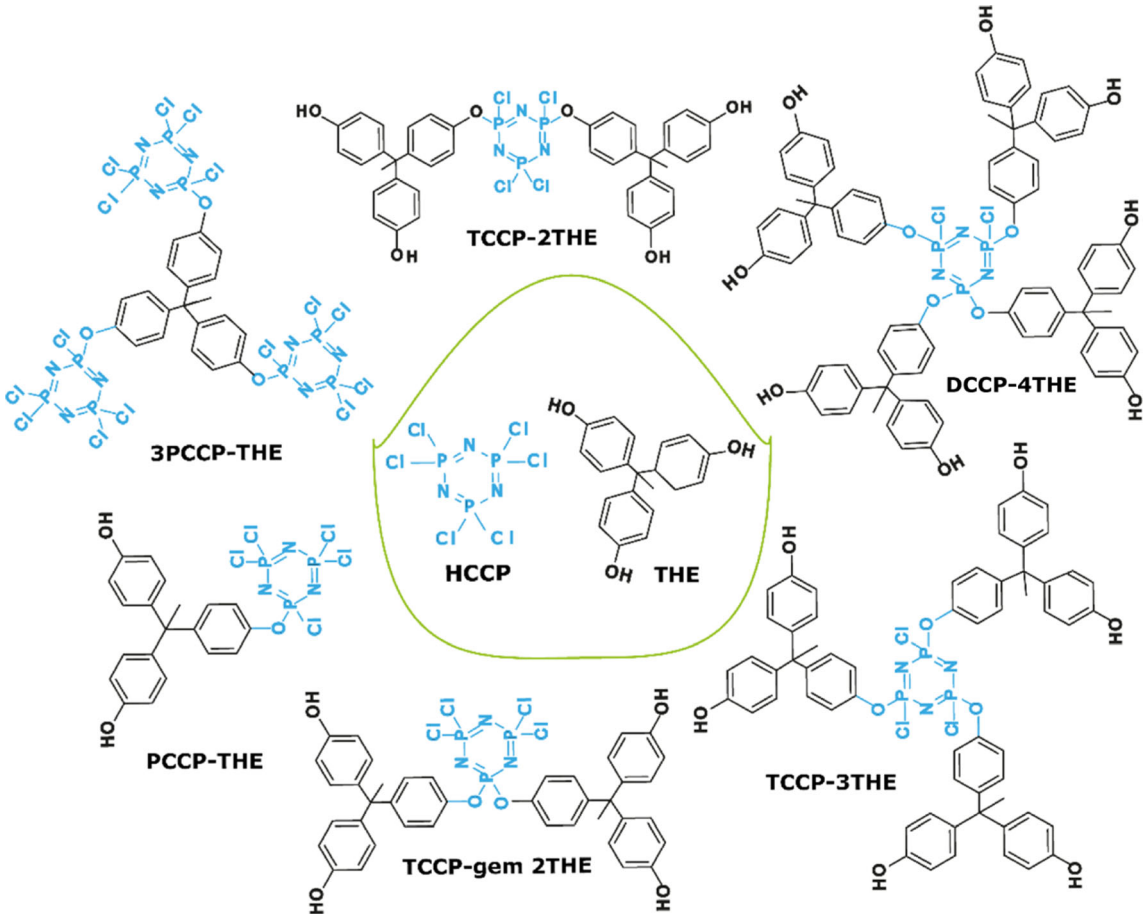

Figure 1 Structures of the studied cyclophosphazene, tris 4–(hydroxyphenyl) ethane and their derived organocyclo–phosphazenes.

The β_{ijk} components were calculated using the finite field approach as implemented in Gaussian 09 [41]. The two properties $\beta_{HRS}(-2\omega;\omega,\omega)$ and $\beta_{//}(-2\omega;\omega,\omega)$ can be deduced from the EFISHG measurements. The $\beta_{HRS}(-2\omega;\omega,\omega)$ is here related to the HRS intensity for non-polarized incident light and observation of plane-polarized scattered light made perpendicularly to the propagation plane. The HRS method allows obtaining different independent tensor components of the first hyperpolarizability, which is not possible by EFISHG [42].

$$\beta_{//}(-2\omega;\omega,\omega) = \beta_{//} = \frac{1}{5}\sum_{i}\frac{\mu_i}{|\vec{\mu}|}\sum_{j}\left(\beta_{ijj}+\beta_{jij}+\beta_{jji}\right) \tag{4}$$

In the static limits, the component $\beta_{ijj} = \beta_{jij} = \beta_{jji}$ and so,

$$\beta_{//} = \frac{3}{5}\sum_{i=x,y,z}\frac{\mu_i\beta_i}{|\vec{\mu}|} \tag{5}$$

$|\vec{\mu}|$ is the norm of the dipole moment.

μ_i and β_i are the ith components of the μ and β vectors, respectively.

In HRS, the depolarization ratios DR were also calculated. For a non-polarized incident signal, and for the reason that both polarizations are detected with equal sensitivity, the orientational average over β is

$$|\beta_{HRS}| = \sqrt{\langle\beta^2_{HRS}\rangle} = \sqrt{\langle\beta^2_{ZZZ}\rangle + \langle\beta^2_{ZXX}\rangle} \tag{6}$$

and

$$DR = \frac{I^{2\omega}_{VV}}{I^{2\omega}_{HV}} = \frac{\langle\beta^2_{ZZZ}\rangle}{\langle\beta^2_{ZXX}\rangle} \tag{7}$$

The $\langle\beta^2_{ZZZ}\rangle$ and $\langle\beta^2_{ZXX}\rangle$ are orientational averages of the β tensor components, describing the HRS

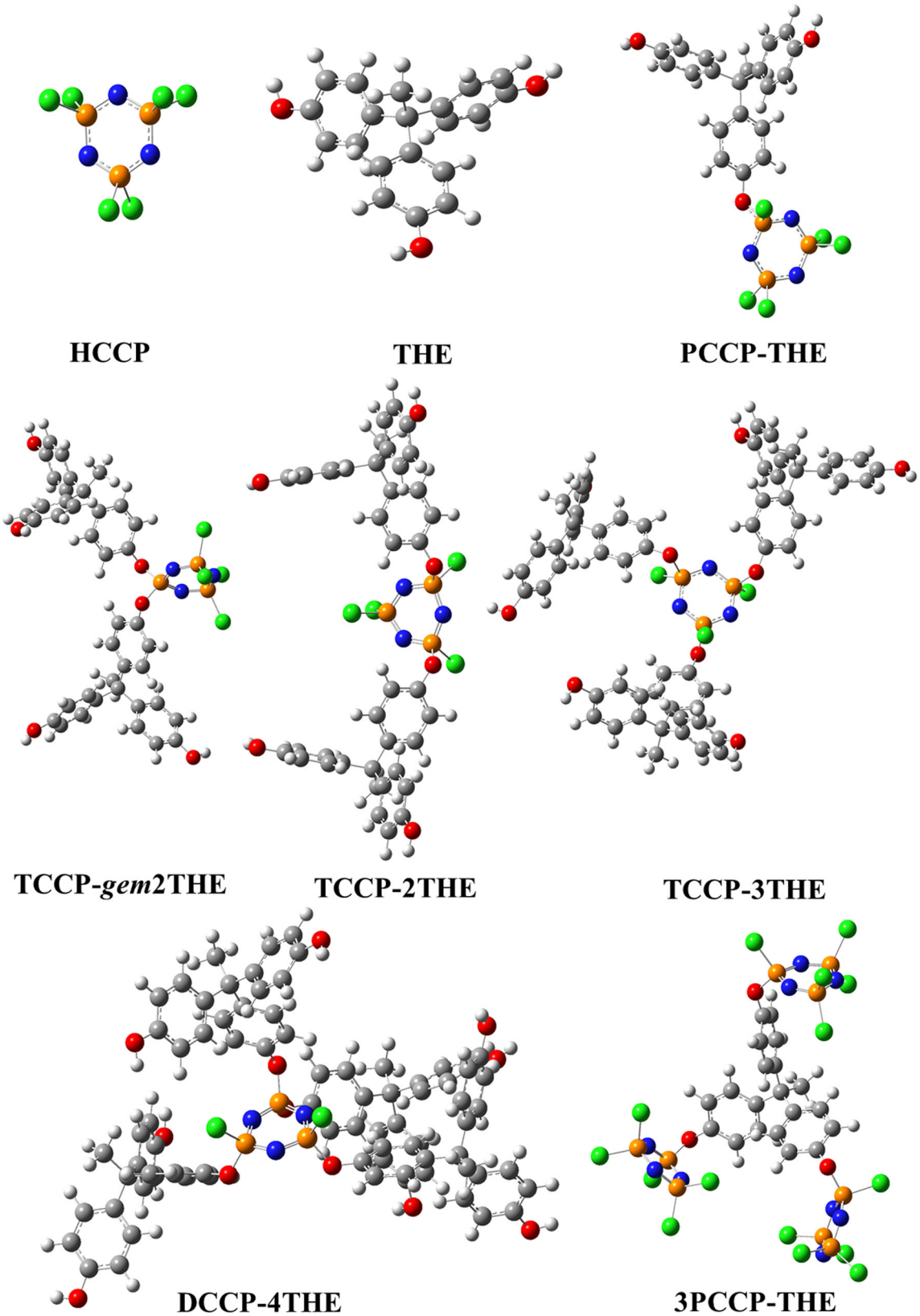

Figure 2 Optimized geometries of the cyclophosphazene and their derived organocyclo–phosphazenes at the B3LYP/6–311 + G(d) level.

intensities when the incident light is vertically or horizontally polarized, respectively. These two invariants $\langle\beta^2_{ZZZ}\rangle$ and $\langle\beta^2_{ZXX}\rangle$ are calculated without assuming Kleinman's conditions. Their full expressions can be find in Ref. [43]

Results and discussions

Linear and NLO properties

Dipole moment

Figure 2 lists the relevant optimized geometries of the studied phosphazenes HCCP, THE, PCCP–THE, TCCP–3THE, TCCP–gem2THE, DCCP–4THE, TCCP–2THE, and 3PCCP–THE optimized at the B3LYP/6–311 + G(d,p) level. In Table 1, we summarize the dipole moment values of our phosphazenes performed at DFT level for the geometry optimized at the B3LYP/6–311 + + G(d,p) level of theory. The accurate calculation of dipole moment, polarizability and first hyperpolarizability requires extended basis sets. Indeed, it is obvious that for the computational reasons, moderate size basis sets are preferable [45–47]. In our study, the choice of these two 6–311 + G(d,p) and aug–cc–pVDZ basis sets is to find a good compromise between precision and calculation needs. Nandi et al. showed in several studies [48–50] of the hyperpolarizability of medium size molecules that the 6–311 + + G(d,p) basis set can give almost identical results of β as obtained with the Dunning's correlation consistent basis set higher angular momentum diffuse functions. High μ values were obtained for the TCCP–3THE and PCCP–THE (Table 1, Fig. 4, and Fig. 5). On the other hand, for TCCP–gem2THE and 3PCCP–THE, low values have been obtained compared to the μ values for the TCCP–3THE and PCCP–THE. Because of their high symmetry confirmed by the D_{3h} symmetry group, and the planar cyclic arrangement [51], the HCCP shows zero μ values. This μ value was confirmed in our recent study [52]. The THE and TCCP–3THE are octupolar by symmetry, and their symmetry group is C_3. In the case of (PCCP–THE, TCCP–gem2THE, TCCP–2THE, DCCP–4THE, and 3PCCP–THE), and after the optimization of geometric structures, the reorientation of THE groups linked to the HCCP cycle creates asymmetric structures of these compounds, and then, these compounds belong to the C_1 point group. The B3LYP and ωB97X–D DFT functionals give the highest μ values in comparison with the M05–2X and CAM–B3LYP functionals (Table 1 and Fig. 3). The B3LYP/aug–cc–pVDZ μ values of the TCCP–3THE which gets the high μ values differ by about 31%, 70%, 14%, 41%, 41%, and 63% for TCCP–2THE, TCCP–gem2THE, PCCP–THE, DCCP–4THE, THE, and 3PCCP–THE, respectively. The obtained μ values at the B3LYP/aug–cc–pVDZ level evolve in the following order: $(\mu = 0)_{HCCP} < \mu_{TCCP-gem2THE} < \mu_{3PCCP-THE} < \mu_{THE} < \mu_{DCCP-4THE} < \mu_{TCCP-2THE} < \mu_{PCCP-THE} < \mu_{TCCP-3THE}$.

Theoretical papers [52, 53] confirmed the null dipole moment for the HCCP. For similar chair-like phosphazenes ($(PHNH)_3$, $(PFNF)_3$, $(PClNCl)_3$ and $(PBrNBr)_3$), theirs μ values ranged from 1.23, 2.28, 2.73, and 3.09 D, respectively. The calculated μ value (3.69 D) for the THE at the CAM–B3LYP/aug–cc–pVDZ level is in close agreement with the theoretical data (3.67 D) showed by Zheng et al. [44] for the diazonaphthoquinone photoactive compound (DNQ PAC)-based THE compound calculated using the PW91 level. For all studied phosphazenes, the augmented correlation consistent basis set aug–cc–pVDZ gives highest μ values compared to the 6–311 + G(d) basis set. Polyphosphazene/polynitrile copolymers present μ comparable to polyphosphazenes, and to the one of standard push–pull systems [54].

Polarizability

In phosphazenes, the highly polarized PN backbone of the phosphazene ring [8], and the direct relation with the ligand electronegativity on the phosphorus atom [54], makes our phosphazenes carry high polarizability values. In the PN bond, the phosphorus d orbitals play a very important role in the formation of the PN bonds. The system $d_\pi(P) - p_\pi(N)$ has been generally accepted and confirmed by several studies [55–57]. From the results presented in Table 1 and Fig. 3, we note that the DFT functionals give higher mean polarizabilities $\langle\alpha\rangle$ and $\Delta\alpha$ values of our studied phosphazenes except the HCCP.

The mean polarizability $\langle\alpha\rangle$ values of our phosphazenes showed that the DCCP–4THE gets the high $\langle\alpha\rangle$ values (1099.41 Arb. Units) compared to other phosphazene compounds. This phosphazene is connected by four THE. Similar trend has been obtained for the 3PCCP–THE, TCCP–gem2THE, and TCCP–

Table 1 B3LYP, ωB97X–D, CAM–B3LYP, and M05–2X dipole moment μ, mean polarizability ⟨α⟩, polarizability anisotropy Δα, EFISHG first hyperpolarizability $\beta_{//}$, HRS first hyperpolarizability β_{HRS}, and the depolarization ratios DR (in parentheses) for the HCCP and their derived materials

		HCCP				THE				
		μ	$\langle\alpha\rangle$	$\Delta\alpha$	β_{HRS}(DR)	μ	$\langle\alpha\rangle$	$\Delta\alpha$	$\beta_{//}$	β_{HRS}(DR)
B3LYP	6–311 + G(d)	0.00	158.55	1.89	80.00 (1.50)	3.03	243.33	73.92	235.35	216.88 (3.26)
	aug–cc–pVDZ	0.00	180.21	1.01	82.41 (1.50)	3.41	264.52	76.23	236.31	226.31 (3.24)
ωB97X–D	6–311 + G(d)	0.00	153.00	0.63	85.83 (1.50)	3.13	237.36	69.95	222.26	234.58 (2.92)
	aug–cc–pVDZ	0.00	175.21	0.22	87.89 (1.50)	3.54	258.65	73.54	224.36	239.62 (2.88)
CAM–B3LYP	6–311 + G(d)	0.00	158.54	0.61	82.39 (1.50)	3.16	238.14	70.01	222.91	214.31 (3.24)
	aug–cc–pVDZ	0.00	179.51	0.24	84.98 (1.50)	3.69	259.68	75.47	225.63	224.75 (3.20)
M05–2X	6–311 + G(d)	0.00	154.13	0.52	81.05 (1.50)	3.18	235.43	69.88	219.62	210.65 (3.18)
	aug–cc–pVDZ	0.00	174.54	0.15	83.56 (1.50)	3.60	251.56	72.00	223.00	221.85 (3.01)
		0.00 [c]				3.67 [b]				
		0.00 [d]								
			114.38[a]							
			113.61[a]							

		PCCP–THE					TCCP–gem2THE				
		μ	$\langle\alpha\rangle$	$\Delta\alpha$	$\beta_{//}$	β_{HRS}(DR)	μ	$\langle\alpha\rangle$	$\Delta\alpha$	$\beta_{//}$	β_{HRS}(DR)
B3LYP	6–311 + G(d)	4.82	395.54	110.18	− 163.22	319.10 (3.64)	1.67	617.45	121.12	3.07	323.96 (4.03)
	aug–cc–pVDZ	4.93	410.32	112.36	− 173.21	329.56 (3.62)	1.71	629.31	124.98	3.23	333.94 (4.05)
ωB97X–D	6–311 + G(d)	4.82	383.41	101.58	− 111.40	338.54 (3.20)	1.66	607.25	112.54	2.98	342.64 (4.12)
	aug–cc–pVDZ	4.92	392.10	109.54	− 121.41	347.45 (3.18)	1.70	617.35	114.54	3.00	353.60 (4.15)
CAM–B3LYP	6–311 + G(d)	4.80	384.26	101.40	− 132.75	321.58 (3.60)	1.65	608.65	112.31	2.97	325.52 (4.08)
	aug–cc–pVDZ	4.89	393.10	108.00	–133.47	330.98 (3.54)	1.69	619.34	114.54	3.01	336.11 (4.11)
M05–2X	6–311 + G(d)	4.79	382.31	100.55	− 155.13	315.74 (3.60)	1.64	606.52	110.58	2.87	321.13 (4.01)
	aug–cc–pVDZ	4.87	390.57	107.58	–166.35	324.58 (3.55)	1.68	615.89	113.65	2.97	332.56 (4.05)

		TCCP–2THE					TCCP–3THE				
		μ	$\langle\alpha\rangle$	$\Delta\alpha$	$\beta_{//}$	β_{HRS}(DR)	μ	$\langle\alpha\rangle$	$\Delta\alpha$	$\beta_{//}$	β_{HRS}(DR)
B3LYP	6–311 + G(d)	3.84	616.66	106.74	320.31	382.74 (2.45)	5.45	665.33	202.47	67.65	354.01 (1.54)
	aug–cc–pVDZ	3.95	627.11	109.56	323.54	401.45 (2.50)	5.78	695.21	225.36	69.42	365.74 (1.56)
ωB97X–D	6–311 + G(d)	3.70	608.87	102.31	310.47	391.54 (2.73)	5.48	661.11	198.54	60.01	374.51 (1.53)
	aug–cc–pVDZ	3.75	618.65	103.87	314.25	395.56 (2.82)	5.84	687.65	215.65	61.45	383.01 (1.57)
CAM–B3LYP	6–311 + G(d)	3.82	617.21	101.65	312.45	384.65 (2.43)	5.39	660.32	197.10	60.85	356.10 (1.54)
	aug–cc–pVDZ	3.90	628.31	104.67	316.56	396.13 (2.51)	5.74	685.56	213.01	62.14	366.32 (1.59)
M05–2X	6–311 + G(d)	3.81	604.25	99.12	309.58	380.94 (2.39)	5.25	659.54	196.32	59.54	351.54 (1.54)
	aug–cc–pVDZ	3.89	614.32	102.57	313.14	390.55 (2.42)	5.58	684.87	212.54	59.01	360.65 (1.57)

		DCCP–4THE					3PCCP–THE				
		μ	$\langle\alpha\rangle$	$\Delta\alpha$	$\beta_{//}$	β_{HRS}(DR)	μ	$\langle\alpha\rangle$	$\Delta\alpha$	$\beta_{//}$	β_{HRS}(DR)
B3LYP	6–311 + G(d)	3.34	1082.83	226.70	263.35	471.67 (4.96)	2.03	638.86	50.48	10.78	100.92 (0.45)
	aug–cc–pVDZ	3.41	1099.41	231.58	267.98	482.65 (4.97)	2.14	659.54	53.65	11.89	119.21 (0.48)
ωB97X–D	6–311 + G(d)	3.45	1072.31	215.65	253.64	491.24 (4.98)	2.12	635.42	48.54	9.54	124.58 (0.43)
	aug–cc–pVDZ	3.49	1079.65	219.61	258.45	497.54 (4.99)	2.18	655.69	52.65	10.68	133.75 (0.47)
CAM–B3LYP	6–311 + G(d)	3.32	1074.25	224.58	264.58	473.56 (4.85)	2.02	640.58	52.32	12.78	102.91 (0.44)
	aug–cc–pVDZ	3.39	1083.56	239.54	268.45	485.75 (4.86)	2.12	662.57	55.89	13.25	121.35 (0.49)

Table 1 continued

		DCCP–4THE					3PCCP–THE				
		μ	$\langle\alpha\rangle$	$\Delta\alpha$	$\beta_{//}$	β_{HRS}(DR)	μ	$\langle\alpha\rangle$	$\Delta\alpha$	$\beta_{//}$	β_{HRS}(DR)
M05–2X	6–311 + G(d)	3.30	1071.21	224.56	260.42	468.45 (4.65)	2.03	636.32	49.01	10.21	109.12 (0.45)
	aug–cc–pVDZ	3.32	1080.59	229.74	264.31	473.65 (4.69)	2.13	647.52	52.00	11.50	117.45 (0.47)

Both 6–311 + G(d) and aug–cc–pVDZ basis sets were used. All results are given in arbitrary units (Arb. Units) and were obtained using the ground state geometry optimized at the B3LYP level

[a][30] for similar cyclic phosphazene (AM1 calculation)

[b][44] for diazonaphthoquinone photoactive compound (DNQ PAC)-based THE compound (PW91 calculation)

[c][51] DFT calculation for HCCP

[d][52] DFT calculation for HCCP

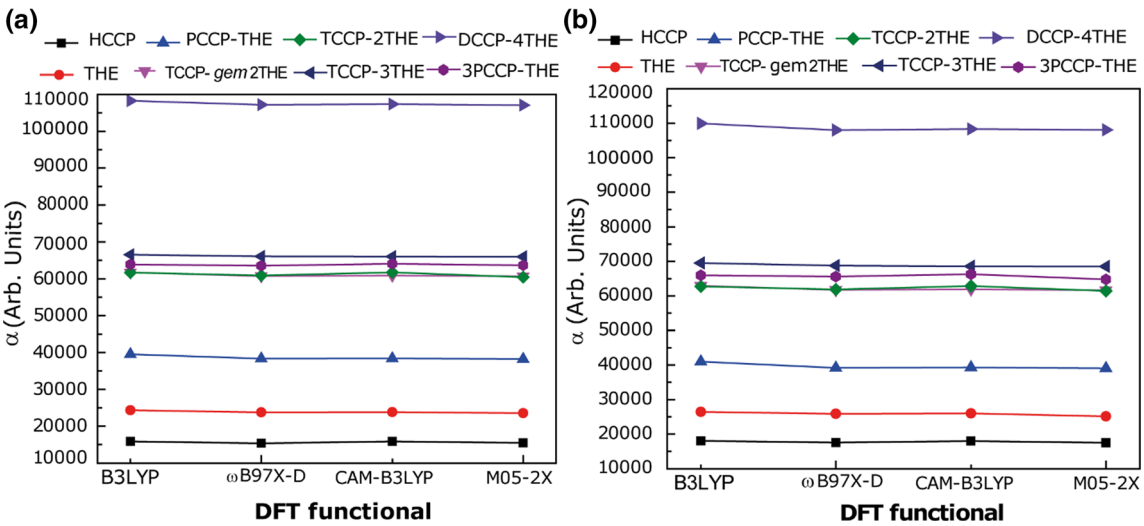

Figure 3 Mean polarizablility $\langle\alpha\rangle$ of HCCP, THE, PCCP–THE, TCCP–gem2THE, TCCP–3THE, TCCP–3THE, DCCP–4THE, and 3PCCP–THE compounds determined at different levels of approximation using the 6–311 + G(d) (**a**) and aug–cc–pVDZ basis set (**b**).

2THE. Their values at the B3LYP/aug–cc–PVDZ level are 638.86, 629.31, and 627.11 Arb. Units, respectively. The B3LYP/aug–cc–PVDZ level gives the high $\langle\alpha\rangle$ values. Theoretical studies [14, 52] show the reliability of the B3LYP functional for the prediction of polarizability for this compounds type. The results show that the number of THE affects the $\langle\alpha\rangle$ values. High $\Delta\alpha$ values (239.54 Arb. Units) have been obtained for the DCCP–4THE using the CAM–B3LYP/aug–cc–PVDZ level. Using the ωB97X–D/aug–cc–PVDZ level, the lowest $\Delta\alpha$ values (0.22 and 52.65 Arb. Units) have been obtained for HCCP and 3PCCP–THE, respectively. A little difference has been obtained for the HCCP values using the DFT levels, and their values ranged from 0.15 to 1.89 Arb. Units. Semi-empirical $\langle\alpha\rangle$ calculation of similar cyclic phosphazenes [30] shows an acceptable agreement to our $\langle\alpha\rangle$ value for the HCCP. The results show that the mean polarizability is driven by the size of the phosphazenes, but the polarizability anisotropy presents more variations as a function of the phosphazenes. Our recent papers [58–61] showed the same assessment. We note that the B3LYP/aug–cc–pVDZ level gives the high $\langle\alpha\rangle$ values compared to other levels used in this study. The calculated $\langle\alpha\rangle$ value of the DCCP–4THE at the B3LYP/aug–cc–pVDZ level which is the high $\langle\alpha\rangle$ value differs by about 40%, 36%¸43%¸42%, 62%, 76%, and 83% for 3PCCP–THE,

TCCP–3THE, TCCP–2THE, TCCP–gem2THE, PCCP–THE, THE, and HCCP, respectively. For Δα, the calculated value of the DCCP–4THE at the same B3LYP/aug–cc–pVDZ level which is the obtained high Δα value differs by about 77%, 3%¸ 53%¸ 46%, 51%, 67%, and 99% for 3PCCP–THE, TCCP–3THE, TCCP–2THE, TCCP–gem2THE, PCCP–THE, THE, and HCCP, respectively. At the same level, the α values evolve in the following order: $\langle\alpha\rangle_{\text{HCCP}} < \langle\alpha\rangle_{\text{THE}} < \langle\alpha\rangle_{\text{PCCP–THE}} < \langle\alpha\rangle_{\text{TCCP–2THE}} < \langle\alpha\rangle_{\text{TCCP–gem2THE}} < \langle\alpha\rangle_{\text{3PCCP–THE}} < \langle\alpha\rangle_{\text{TCCP–3THE}} < \langle\alpha\rangle_{\text{DCCP–4THE}}$ and $\Delta\alpha_{\text{HCCP}} < \Delta\alpha_{\text{3PCCP–THE}} < \Delta\alpha_{\text{THE}} < \Delta\alpha_{\text{TCCP–2THE}} < \Delta\alpha_{\text{PCCP–THE}} < \Delta\alpha_{\text{TCCP–2THE}} < \Delta\alpha_{\text{TCCP–3THE}} < \Delta\alpha_{\text{DCCP–4THE}}$.

Hyperpolarizability

The results shown in Table 1 present gas phase EFISHG $\beta_{//}$, the HRS first hyperpolarizability β_{HRS} and the depolarization ratios (DR) for all investigated compounds; the values of the hyperpolarizability contributions of Gaussian 09 output are reported in Arb. Units.

The passage from the traditional B3LYP functional to the long-range functional CAM–B3LYP increased the hyperpolarizability β_{HRS} of these compounds by 0.5 to 3% (Fig. 4 and Fig. 5). Comparing the obtained β_{HRS} values using the B3LYP and CAM–B3LYP levels at the same 6–311 + G(d) basis set, the β_{HRS} are increased from (382.74 to 384.65 Arb. Units) and from (354.01 to 356.10 Arb. Units) for the TCCP–2THE and TCCP–3THE, respectively. It is now well recognized that the electron correlation may strongly influence the values of hyperpolarizability [62–66]. The $\beta_{//}$ and β_{HRS} results show also that M05–2X values using aug–cc–pVDZ basis set are higher. Further, it is surprising that the choice of the DFT functional is very required to get the correct tendency of β. According to the phosphazenes surveyed in Table 1, Fig. 4, and Fig. 5, there is little difference among the β_{HRS} values calculated using the B3LYP, CAM–B3LYP, and M05–2X functionals, while the ωB97X–D level shows a somewhat greater propensity to deliver results divergent from these DFT levels. For $\beta_{//}$, there is also little difference between the calculated values using the B3LYP, CAM–B3LYP, and M05–2X functionals, while the ωB97X–D shows a weaker propensity except for PCCP–THE where the difference is clearly marked. The calculated β_{HRS} value of the DCCP–4THE at the ωB97X–D/aug–cc–pVDZ level which is the obtained high β_{HRS} value differs by about 20%, 23%¸ 29%¸ 30%, 52%, 73%, and 82% for TCCP–2THE, TCCP–3THE, TCCP–gem2THE, PCCP–THE, THE, 3PCCP–THE, and HCCP, respectively. For $\beta_{//}$, and at the same ωB97X–D/aug–cc–pVDZ level, the calculated $\beta_{//}$ value of the TCCP–2THE differs by about 18%, 28%¸ 80%¸ 96%, 99%, 100%, and 167% for DCCP–4THE, THE, TCCP–3THE, 3PCCP–THE, TCCP–gem2THE, HCCP, and PCCP–THE, respectively. We can note that at the ωB97X–D/aug–cc–pVDZ level, the β_{HRS} decreases in the order: $\beta_{\text{HRS DCCP–4THE}} > \beta_{\text{HRS TCCP–2THE}} > \beta_{\text{HRS TCCP–3THE}} > \beta_{\text{HRS}} > \beta_{\text{HRS PCCP–THE}} > \beta_{\text{HRS THE}} > \beta_{\text{HRS 3PCCP–THE}} > \beta_{\text{HRS}}$

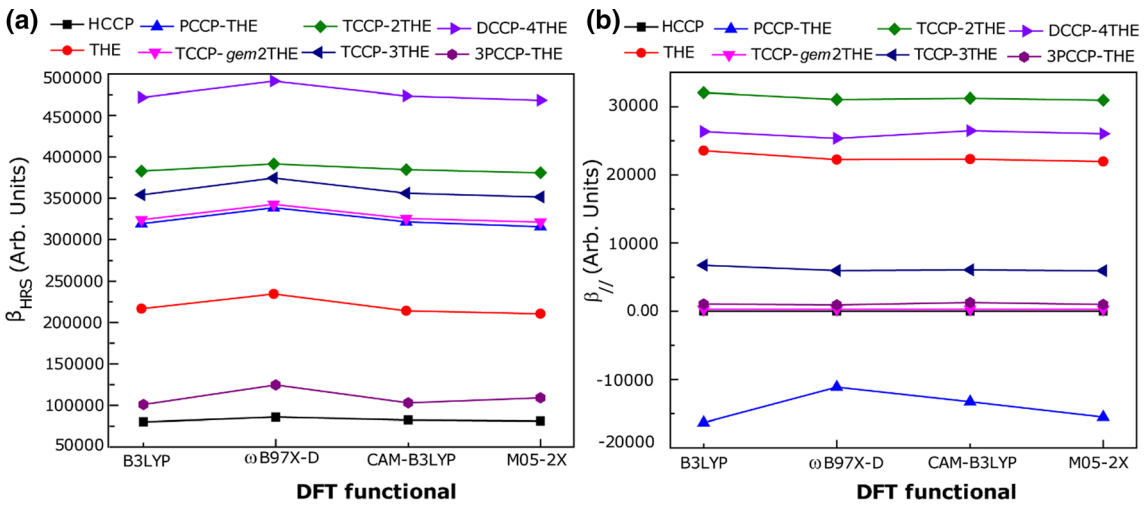

Figure 4 β_{HRS} (**a**) and $\beta_{//}$ (**b**) of HCCP, THE, PCCP–THE, TCCP–gem2THE, TCCP–3THE, TCCP–3THE, DCCP–4THE, and 3PCCP–THE compounds determined at different levels of approximation using the 6–311 + G(d) basis set.

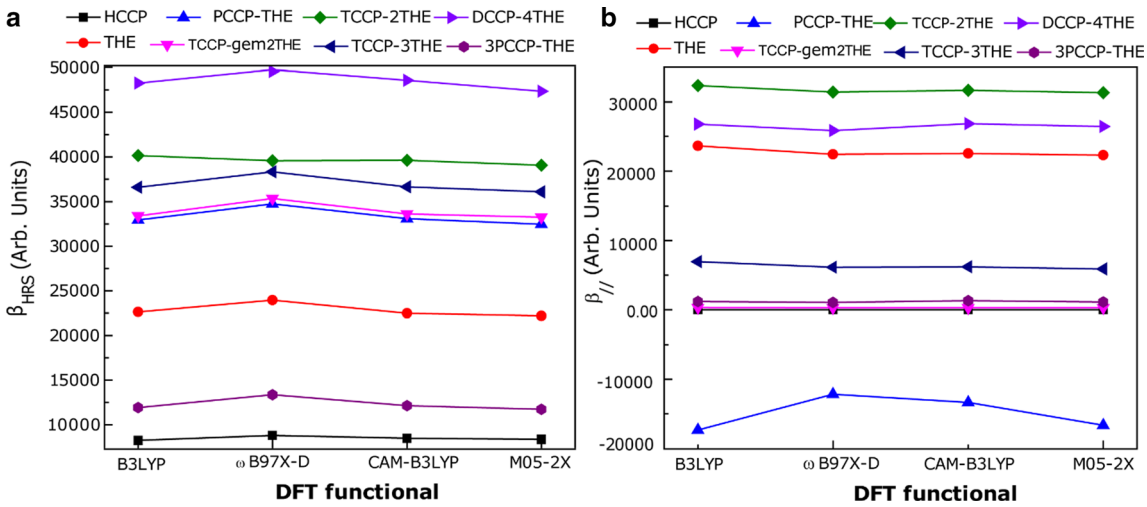

Figure 5 β_{HRS} (**a**) and $\beta_{//}$ (**b**) of HCCP, THE, PCCP–THE, TCCP–gem2THE, TCCP–3THE, TCCP–3THE, DCCP–4THE, and 3PCCP–THE compounds determined at different levels of approximation using the aug–cc–pVDZ basis set.

$_{HCCP}$ and the $\beta_{//}$ decreases in the order: $\beta_{//\ TCCP-2THE} > \beta_{//\ DCCP-4THE} > \beta_{//\ THE} > \beta_{//\ TCCP-3THE} > \beta_{//\ 3PCCP-THE} > \beta_{//\ TCCP-gem2THE} > (\beta_{//} = 0)_{\ HCCP} > \beta_{//\ PCCP-THE}$.

The results from our calculations for the gas phase EFISHG $\beta_{//}$ and the HRS first hyperpolarizability β_{HRS} suggest these compounds as a potential compound for NLO applications. Dendritic NLO chromophores-based THE have been synthesized by Choi et al. [67]; the authors showed that these compound-based THE are thermally stable up to 275 °C in a nitrogen atmosphere, showed as large as 19 pm/V electro–optic coefficient for the poled film and had a glass transition temperature of 76 °C. The dependence between the dipole moment μ and the hyperpolarizability β (M05–2X with the two 6–311 + G(d) and aug–cc–pVDZ basis sets shown in Table 1) is well established. Indeed, a high value of the first-order hyperpolarizability β corresponds to a high value of the dipole moment μ. This high value of the first-order hyperpolarizability β gives rise to large second-order effects, which has applications in electro-optic devices. There is not a large difference between the two functionals CAM–B3LYP and M05–2X for the values of all calculated properties. Several theoretical [53] and experimental [68, 69] studies show the efficiency of phosphazenes for NLO applications. Jacquemin has shown the efficiency of polyphosphazene polynitrile alternating copolymers in their theoretical study [53], using the Møller–Plesset perturbation theory MP2 with the 6–31G(d) basis set. He reported the evolution with the chain length of the geometry, charges, dipole moments, polarizability, and first hyperpolarizability. Theirs results showed that the polyphosphazene copolymers present larger dipole moment, polarizability, and first hyperpolarizability. Li et al. [69] showed that polyphosphazenes containing indole-based dual chromophores have demonstrated the second order NLO property. Our theoretical study is likely to be of value in guiding subsequent efforts toward the reliable predictive calculation of linear and NLO responses for multifunctional phosphazenes-based cyclotriphosphazene of interest to experimentalists. It appears through the study of this series of phosphazenes that the symmetry plays a lot on the NLO response of compounds. Indeed, the depolarization ratios DR cover a broad range of dipolar and octupolar characters, which is directly depends on the symmetry. For our studied phosphazenes, the HCCP and TCCP–3THE are octupolar by symmetry, and their symmetry groups are D_{3h} and C_3, respectively. The DR is exactly equal to 1.5 for HCCP and close to 1.5 for TCCP–3THE. The THE is octupolar by symmetry with C_3 symmetry group, and present intermediate values varied from 2.8 to 3.2. The dominant hyperpolarizability component for octupolar molecule is β_{xyz}, which is in good agreement with our β_{xyz} and DR values. The 3PCCP–THE gets the lowest DR values (DR = 0.45 to 0.5) at the four DFT levels using the 6–311 + G(d) and aug–cc–pVDZ basis sets. The dipolar character of the TCCP–gem2THE increase when adding a THE group

(DCCP–4THE), their DR values are ranged from 4.05 to 4.05. For the PCCP–THE, and compared to HCCP, the octupolar character decreases when adding a THE group (DR = 3.18 to 3.64). The TCCP–2THE present intermediate values (DR = 2.45 to 2.82), it is dominantly octupolar.

Frontier Molecular Orbitals (FMOs) and their energy gaps

The largest and smallest values of the gaps are obtained for HCCP and TCCP–3THE, respectively (Table 2 and Table 3). The corresponding gaps and β_{HRS} values are 5.72, 81.05 and 3.15 eV, 383.01 Arb. Units, respectively. Good agreement has been obtained between our energy gap value obtained at the M05–2X/aug–cc–pVDZ level for the HCCP (Table 2) and that obtained by Zoghaib et al. [70], the difference is 6%. The deviations with respect to experiment reported in our recent paper [71] amount to 15%. Direct correlation has been found between the energy gaps and β_{HRS}. The results show an inverse relationship between the Δε and β_{HRS}. Similar studies show the same finding [59, 72–76].

The shapes of the LUMO orbital have a π character, and their electron density is centered on the cyclotriphosphazene ring in all studied derivatives (Fig. 6). For the HOMO orbital, the delocalization of the molecular orbital appeared mostly on the tris(4–hydroxyphenyl) ethane group in all the studied compounds (Fig. 6). This suggests the important role of the cyclotriphosphazene ring in the optical properties of its partially substituted derivatives. The intramolecular charge transfer process guaranteed formed in large conjugated system like in the case of the DCCP–4THE. In addition, the results show that correlations are found between the increases of the β_{HRS} values and the changes of the isosurfaces of the HOMO and the LUMO for these phosphazenes. The LUMO in the case of DCCP–4THE has a more diffuse on central cyclotriphosphazene and the adjacent

Table 2 The HRS first hyperpolarizability β_{HRS} in Arb

	B3LYP	ωB97X–D	CAM–B3LYP	M05–2X	Exp
HCCP					
β_{HRS}	82.41	87.89	84.98	81.05	
E_{HOMO}	− 8.50	− 8.19	− 8.26	− 8.62 − 8.55 [a]	
E_{LUMO}	− 2.82	− 2.79	− 2.83	− 2.9 − 2.81[a]	
Δε	5.68	5.40	5.43	5.72 5.74 [a]	4.80 [b]
THE					
β_{HRS}	226.31	239.62	224.75	221.85	
E_{HOMO}	− 5.96	− 5.68	− 5.78	− 5.99	
E_{LUMO}	− 0.77	− 0.66	− 0.69	− 0.75	
Δε	5.19	5.02	5.09	5.24	
PCCP–THE					
β_{HRS}	329.56	347.45	330.98	324.58	
E_{HOMO}	− 6.27	− 6.02	− 6.12	− 6.37	
E_{LUMO}	− 2.34	− 2.57	− 2.62	− 2.40	
Δε	3.93	3.45	3.50	3.97	
TCCP–gem2THE					
β_{HRS}	330.25	339.43	322.21	329.89	
E_{HOMO}	− 6.23	− 6.20	− 6.27	− 6.29	
E_{LUMO}	− 2.53	− 2.50	− 2.48	− 2.49	
Δε	3.76	3.70	3.79	3.80	

Units and the energy gaps (Δε in eV) for the HCCP, THE, PCCP–THE, and TCCP–3THE obtained at the four DFT functionals using the aug–cc–pVDZ basis set

[a][70] HCCP energy gap at B3LYP/6–311 + G(d,p)

[b][71] HCCP experimental energy gap from absorbance edge

Table 3 The HRS first hyperpolarizability β_{HRS} in Arb

	B3LYP	ωB97X–D	CAM–B3LYP	M05–2X
TCCP–2THE				
β_{HRS}	399.19	392.44	393.00	388.31
E_{HOMO}	− 6.14	− 6.16	− 6.15	− 6.18
E_{LUMO}	− 2.69	− 2.67	− 2.64	− 2.65
Δε	3.45	3.49	3.51	3.53
TCCP–3THE				
β_{HRS}	365.74	383.01	366.32	360.65
E_{HOMO}	− 6.20	− 5.97	− 6.10	− 6.25
E_{LUMO}	− 2.7	− 2.82	− 2.84	− 2.71
Δε	3.50	3.15	3.26	3.54
DCCP–4THE				
β_{HRS}	478.61	494.52	481.33	470.41
E_{HOMO}	− 6.00	− 5.97	− 5.99	− 6.04
E_{LUMO}	− 2.60	− 2.59	− 2.60	− 2.63
Δε	3.40	3.38	3.39	3.41
3PCCP− THE				
β_{HRS}	117.19	131.87	119.01	115.89
E_{HOMO}	− 7.49	− 7.20	− 7.37	− 7.40
E_{LUMO}	− 2.09	− 1.99	− 2.00	− 1.98
Δε	5.40	5.21	5.37	5.42

Units and the energy gaps (Δε in eV) for the TCCP–2THE, TCCP–3THE, DCCP–4THE, and 3PCCP–THE obtained at four DFT functionals using the aug–cc–pVDZ basis set

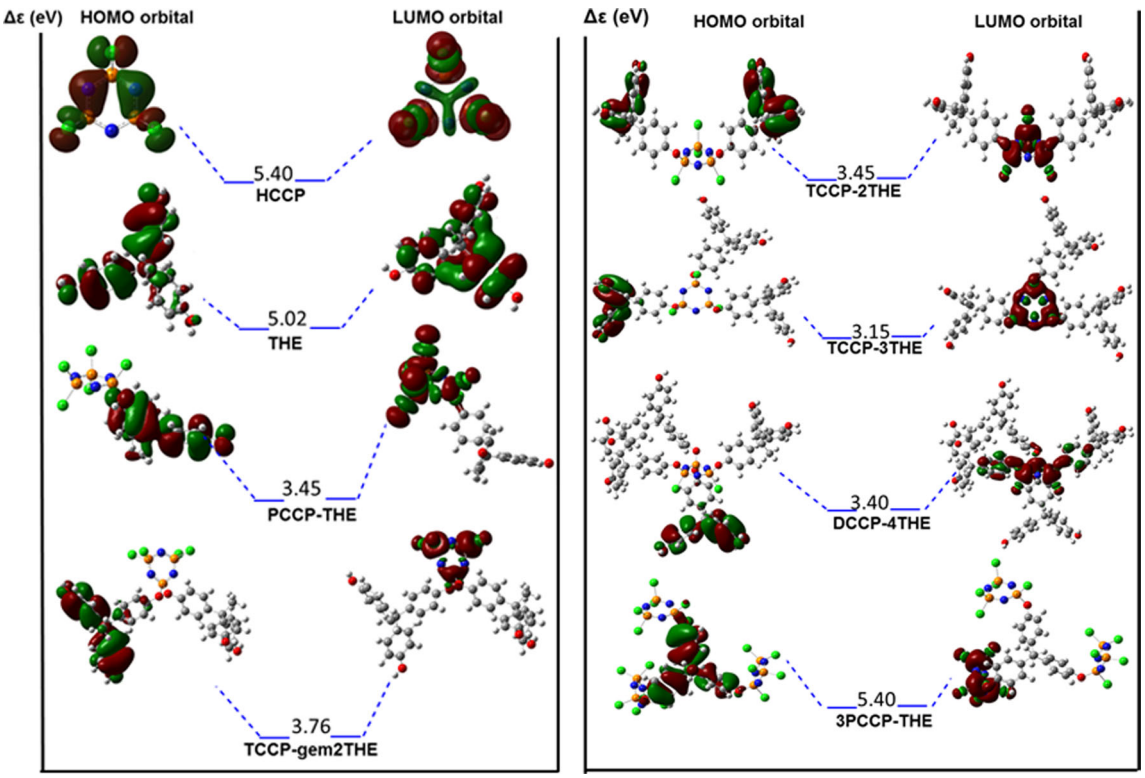

Figure 6 HOMO and LUMO orbitals of the HCCP, THE, PCCP–THE, TCCP–gem2THE, TCCP–2THE, TCCP–3THE, DCCP–4THE, and 3PCCP–THE and their Δε (in eV) estimated by the B3LYP/aug–cc–pVDZ level.

carbon atoms, which correlates with the higher β_{HRS} value compared to other studied phosphazenes. The isosurface of the HOMO of PCCP–THE is almost identical to that obtained in THE which is also consistent as small β_{HRS} values. Our findings are contrast with earlier theoretical results [77] using the CAM–B3LYP/aug–cc–PVDZ, which showed that the HOMO of Li@B10H14 is identical to that of B10H14 and corresponds to small β_{HRS}.

Conclusion

To discover the possibilities of phosphazenes in NLO application, we have studied electrical properties such as dipole moment μ, polarizability α, and first-order hyperpolarizability β for the THE, PCCP–THE, TCCP–3THE, TCCP–gem2THE, and DCCP–4THE selected phosphazenes. DFT studies were performed (B3LYP, CAM–B3LYP, ωB97X–D, and M05–2X functionals) extensively to study and comprehend the change in frontier molecular orbital HOMO and LUMO and their gaps of these compounds. Our results show different values from one to another DFT functionals. The calculations are made on isolated molecules and do not take into account the influence of the environment. However, the β values are strongly influenced by the surrounding solvent [78, 79]. According to the simulations that are made on these phosphazenes, we can predict if one phosphazene will be better than another, which is already very interesting for directing the synthesis toward more efficient molecules in nonlinear optic. The phosphazenes TCCP–3THE, PCCP–THE, DCCP–4THE, and TCCP–gem2THE get the high β_{HRS} compared to other phosphazenes. The HCCP could not attain optical nonlinearities as high compared to other phosphazenes. The DR values of the HCCP and TCCP–3THE are exactly equal to 1.5, which are congruent with their chemical topology. An inverse relationship between the β_{tot} and the gap|HOMO − LUMO| was obtained. The most effective of these phosphazenes are those which have a shorter band gap. To increase the second-order molecular NLO properties for these phosphazenes, a method consists in probing the push–pull disposition to design good NLO chromophores. This strategy was carried out in several studies [80, 81]. This study will provide new direction to the design of new materials for the NLO technologies and their applications.

Declarations

Conflict of interest The authors declare no conflict of interest.

References

[1] Qi L, Sehgal A, Castaing JC, Chapel JP, Fresnais J, Fresnais J, Berret JF, Cousin F (2008) Redispersible hybrid nanopowders: Cerium oxide nanoparticle complexes with phosphonated–peg oligomers. ACS Nano 2:879–888. https://doi.org/10.1021/nn700374d

[2] Shephar JJ, Dickie SA, McQuillan AJ (2010) Structure and conformation of methyl–terminated poly(ethylene oxide)–bis[methylenephosphonate] ligands adsorbed to boehmite (ALOOH) from aqueous solutions attenuated total reflection infrared (ATR–IR) spectra and dynamic contact angles. Langmuir 26:4048–4056. https://doi.org/10.1021/la903506q

[3] Tromsdorf UI, Bruns OT, Salmen SC, Beisiegel U, Weller H (2009) A Highly effective, nontoxic T1 MR contrast agent based on ultrasmall PEGylated iron oxide nanoparticles. Nano Lett 9:4434–4440. https://doi.org/10.1021/nl902715v

[4] White MA, Johnson JA, Koberstein JT, Turro NJ (2006) Toward the syntheses of universal ligands for metal oxide surfaces: controlling surface functionality through click chemistry. J Am Chem Soc 128:11356–11357. https://doi.org/10.1021/ja064041s

[5] Boyer C, Bulmus V, Priyanto P, Teoh WY, Amal R, Davis TP (2009) The stabilization and bio–functionalization of iron oxide nanoparticles using heterotelechelic polymers. J Mater Chem 19:111–123. https://doi.org/10.1039/B815202K

[6] Quéffelec C, Petit M, Janvier P, Knight DA, Bujoli B (2012) Surface modification using phosphonic acids and esters. Chem Rev 112:3777–3807. https://doi.org/10.1021/cr2004212

[7] Kamiya T, Hemmi K, Takeno H, Hascimoto M (1980) Studies on phosphonic acid antibiotics. I. Structure and synthesis of 3–(n–acetyl–n–hydroxyamino) propylphosphonic acid (FR–900098) and its n–formyl analogue (FR–31564). Tetrahedron Lett 21:95–98. https://doi.org/10.1016/S0040-4039(00)93633-5

[8] Dake LS, Baer DR, Ferris KF, Friedrich DM (1990) Ligand and structure effects on the N-P bonds of phosphazenes. J Electron Spectrosc 51:439–457. https://doi.org/10.1016/0368-2048(90)80173-8

[9] Allcock HR (1976) Polyphosphazenes: new polymers with inorganic backbone atoms. Science 193:1214–1219. https://doi.org/10.1126/science.193.4259.1214

[10] Allcock HR (1986) Poly(organophosphazenes): synthesis, unique properties, and applications. Makromol Chem Macromol Symp 6:101–108. https://doi.org/10.1002/masy.19860060112

[11] Allcock HR, Dembek AA, Kim C, Devine RLS, Shi Y, Steier WH, Spangler CW (1991) Second–order nonlinear optical poly(organophosphazenes): synthesis and nonlinear optical characterization. Macromolecules 24:1000–1010. https://doi.org/10.1021/ma00005a006

[12] Maturana RG, Valenzuela ML, Schott E, Rojas-Poblete M (2017) Bonding and optical properties of spirocyclic–phosphazene derivatives A DFT approach. Phys Chem Chem Phys 19:31479–31486. https://doi.org/10.1039/C7CP06064E

[13] Jha PC, Krishnan A, Das PK, Ramasesha S (2002) Nonlinear optical properties of linear chain phosphazenes, (PN)x. J Chem Phys 117:2873. https://doi.org/10.1063/1.1491878

[14] Hadji D (2021) Phosphates branching effect on the structure, linear and NLO properties of linear phosphazenes. Mater Chem Phys 262:124280. https://doi.org/10.1016/j.matchemphys.2021.124280

[15] Allcock HR, Primrose AP, Silverberg EN, Visscher KB, Rheingold AL, Guzei IA, Parvez M (2000) Synthesis and Crystal Structure of Tris(9,10–phenanthrenedioxy) cyclotriphosphazene. A new clathration system. Chem Mater 12:2530–2536. https://doi.org/10.1021/cm990381j

[16] Comotti A, Gallazzi MC, Simonutti R, Sozzani P (1998) ^{13}C and ^{31}P magic-angle spinning nuclear magnetic resonance spectroscopy of tris(2,3–naphthalenedioxy)cyclotriphosphazene inclusion compounds. Chem Mater 10:3589–3596. https://doi.org/10.1021/cm980338g

[17] Sozzani P, Comotti A, Simonutti R, Meersmann T, Logan JW, Pines A (2000) A porous crystalline molecular solid explored by hyperpolarized xenon. Angew Chem Int Ed 39:2695–2699. https://doi.org/10.1002/1521-3773(20000804)39:15%3c2695::AID-ANIE2695%3e3.0.CO;2-M

[18] Carriedo GA, Alonso FJG, García JL, Carbajo RJ, Ortiz FL (1999) Synthesis and ^{1}H–, ^{15}N–, ^{31}P–, ^{183}W–multinuclear magnetic resonance study of the cyclotriphosphazenes [N_3P_3(dobp)$_2$(OC_5H_4N–4)$_2$] and [N_3P_3(dobp)(OC_5H_4N–4)$_4$] and their W(CO)$_5$ complexes (dobp = 2,2′–dioxybiphenyl). Eur J Inorg Chem 1999:1015–1020. https://doi.org/10.1002/(SICI)1099-0682(199906)1999:6%3c1015::AID-EJIC1015%3e3.0.CO;2-X

[19] Kuan JF, Lin KF (2004) Synthesis of hexa-allylamino-cyclotriphosphazene as a reactive fire retardant for unsaturated polyesters. J Appl Polym Sci 91:697–702. https://doi.org/10.1002/app.13044

[20] Allcock HR, McDonnell GS, Riding GH, Manners I (1990) Influence of different organic side groups on the thermal behavior of polyphosphazenes: random chain cleavage, depolymerization, and pyrolytic cross–linking. Chem Mater 2:425–432. https://doi.org/10.1021/cm00010a021

[21] Bowmer TN, Haddon RC, ChichesterHicks S, Gomez MA, Marco C, Fatou JG (1991) Effect of substituents on the thermal transitions and degradation behavior of poly[bis(R–phenoxy)phosphazenes]. Macromolecules 24:4827. https://doi.org/10.1021/ma00017a016

[22] Devaraju S, Selvi M, Alagar M (2018) Synthesis and characterization of thermally stable and flame retardant hexakis(4–aminophenoxy)cyclotriphosphazene–based polyimide matrices. Int J Polym Anal Charact 23:29–37. https://doi.org/10.1080/1023666X.2017.1387021

[23] Allcock HR, Siegel LA (1964) Phosphonitrilic compounds. III.1 molecular inclusion compounds of tris(o–phenylenedioxy)phosphonitrile trimer. J Am Chem Soc 86:5140–5144. https://doi.org/10.1021/ja01077a019

[24] Hertzsch T, Budde F, Weber E, Hulliger J (2002) Supramolecular-wire confinement of I2 molecules in channels of the organic zeolite tris(o–phenylenedioxy)cyclotriphosphazene. Angew Chem Int Ed 41:2281–2284. https://doi.org/10.1002/1521-3773(20020703)41:13%3c2281::AID-ANIE2281%3e3.0.CO;2-N

[25] Y. Xia, C. Zhan, J. Qin, D. Liu, B. Wu, C. Chen, Synthesis and SHG effect of some cyclotriphosphazene derivatives, Proc. SPIE 3556, Electro–Optic and Second Harmonic generation materials, devices, and applications II, 3556 (1998) 16–19. https://doi.org/10.1117/12.318233

[26] Zhang L, Shi J, Jiang ZW, Huang MM, Chen ZJ, Gong QH, Cao SK (2008) Photorefractive performance of hyperstructured cyclotriphosphazene molecular glasses containing carbazole moieties. Adv Funct Mater 18:362–368. https://doi.org/10.1002/adfm.200700257

[27] Kim K (2007) Synthesis of nonlinear optical hexakis(4–carboxyphonoxy)cyclotriphosphazene. Polym Korea 04:85–85

[28] Kang L, Zhang X, Liang F, Lin Z, Huang B (2019) Poly(difluorophosphazene) as the first deep–Ultraviolet nonlinear optical polymer: a first–principles prediction. Angew Chem 131:10356–10360. https://doi.org/10.1002/ange.201905025

[29] Allcock HR, Cameron CG, Skloss TW, Taylor-Meyers S, Haw JF (1996) Molecular motion of phosphazene–bound nonlinear optical chromophores. Macromolecules 29:233–238. https://doi.org/10.1021/ma950452+

[30] Ferris KF, Samuels WD, Morita Y, Exarhos GJ (1994) Solution chemistry effects on the nonlinear optical properties of phosphazenes. Mater Res Soc Symp Proc 374:217–223. https://doi.org/10.1557/PROC-374-217

[31] Basharat M, Liu W, Zhang S, Abbas Y, Wu Z, Wu D (2019) Poly(cyclotriphosphazene–co–tris(4–hydroxyphenyl)ethane) microspheres with intrinsic excitation wavelength tunable multicolor photoluminescence. Macromol Chem Phys 220:1900256. https://doi.org/10.1002/macp.201900256

[32] Becke AD (1988) Density–functional exchange–energy approximation with correct asymptotic behavior. J Phys Rev A 38:3098. https://doi.org/10.1103/PhysRevA.38.3098

[33.] Lee C, Yang W, Parr RG (1988) Development of the Colle-Salvetti correlation–energy formula into a functional of the electron density. Phys Rev B 37:785–789. https://doi.org/10.1103/PhysRevB.37.785

[34] Yanai T, Tew DP, Handy NC (2004) A new hybrid exchange–correlation functional using the Coulomb–attenuating method (CAM–B3LYP). J Chem Phys Lett 393:51–57. https://doi.org/10.1016/j.cplett.2004.06.011

[35] Iikura H, Tsuneda T, Yanai T, Hirao K (2001) A long–range correction scheme for generalized–gradient–approximation exchange functionals. J Chem Phys 115:3540. https://doi.org/10.1063/1.1383587

[36] Zhao Y, Schultz NE, Truhlar DG (2006) Design of density functionals by combining the method of constraint satisfaction with parametrization for thermochemistry, thermochemical kinetics, and noncovalent interactions. J Chem Theory Comput 2:364. https://doi.org/10.1021/ct0502763

[37] Zhao Y, Truhlar DG (2008) The M06 suite of density functionals for main group thermochemistry, thermochemical kinetics, noncovalent interactions, excited states, and transition elements: two new functionals and systematic testing of four M06–class functionals and 12 other functionals. Theor Chem Acc 120:215. https://doi.org/10.1007/s00214-007-0310-x

[38] Suponitsky KY, Tafur S, Masunov AE (2008) Applicability of hybrid density functional theory methods to calculation of molecular hyperpolarizability. J Chem Phys 129:044109. https://doi.org/10.1063/1.2936121

[39] Suponitsky KY, Masunov AE, Antipin MY (2008) Conformational dependence of the first molecular hyperpolarizability in the computational design of nonlinear optical materials for optical switching. Mendeleev Commun 18:265–267. https://doi.org/10.1016/j.mencom.2008.09.013

[40] Suponitsky KY, Liao Y, Masunov AE (2009) Electronic Hyperpolarizabilities for donor-acceptor molecules with long conjugated bridges: calculations versus experiment. J Phys Chem A 113:10994–11001. https://doi.org/10.1021/jp902293q

[41] Frisch MJ et al (2009) Gaussian09, revision C.01. Gaussian Inc., Wallingford

[42.] Castet F, Bogdan E, Plaquet A, Ducasse L, Champagne B, Rodriguez V (2012) Referencemolecules for nonlinear optics: a joint experimental and theoretical investigation. J Chem Phys 136:024506. https://doi.org/10.1063/1.3675848

[43] Bersohn R, Pao YH, Frisch HL (1966) Double quantum light scattering by molecules. J Chem Phys 45:3184. https://doi.org/10.1063/1.1728092

[44] Zheng F, van Sittert CGCE, Lu Q (2017) A computational probe into dissolution inhibitation effect of diazonaphthoquinone photoactive compounds on positive tone photosensitive polyimides. J Phys Chem C 121:1704–1714. https://doi.org/10.1021/acs.jpcc.6b11316

[45] Alam MM, Kundi V, Thankachan PP (2016) Solvent effects on static polarizability, static first hyperpolarizability and one– and two–photon absorption properties of functionalized triply twisted Möbius annulenes: a DFT study. Phys Chem Chem Phys 18:21833–21842. https://doi.org/10.1039/C6CP02732F

[46] Balakina MY, Nefediev SE (2007) The choice of basis set for calculations of linear and nonlinear optical properties of conjugated organic molecules in gas and in dielectric medium by the example of p–nitroaniline. Comput Mater Sci 38:467–472. https://doi.org/10.1016/j.commatsci.2005.05.011

[47] Avci D, Bas A, Lu O, Atalay Y (2011) Effects of different basis sets and donor-acceptor groups on linear and second-order nonlinear optical properties and molecular frontier orbital energies. Int J Quantum Chem 111:130–147. https://doi.org/10.1002/qua.22416

[48] Roy RS, Nandi PK (2015) Exploring bridging effect on first hyperpolarizability. RSC Adv 5:103729–103738. https://doi.org/10.1039/C5RA22615E

[49] Hatua K, Nandi PK (2013) Beryllium–cyclobutadiene multidecker inverse sandwiches: electronic structure and second–hyperpolarizability. J Phys Chem A 117:12581–12589. https://doi.org/10.1021/jp407563f

[50] Hatua K, Nandi PK (2014) Double coned inverse sandwich complexes [M–(η4–C_4H_4)–M′] of Gr–IA and Gr–IIA Metals: theoretical study of electronic of structure and second hyperpolarizability. J Mol Model 20:2440–2449. https://doi.org/10.1021/j100025a017

[51] Kupka T, Pasterny K, Pasterna G, Brandt K (2008) From planar to nonplanar cyclotriphosphazenes. J Molecul Struct (Theochem) 866:21–26. https://doi.org/10.1016/j.theochem.2008.06.032

[52] Hadji D, Rahmouni A (2016) Molecular structure, linear and nonlinear optical properties of some cyclic phosphazenes: a

theoretical investigation. J Mol Struct 1106:343–351. https://doi.org/10.1016/j.molstruc.2015.10.033

[53] Jacquemin D (2005) Linear and nonlinear optics properties of polyphosphazene/polynitrile alternating copolymers. J Chem Theory Comput 1:307–314. https://doi.org/10.1021/ct049884t

[54] Ferris KF, Friedman P, Friedrich DM (1988) Electronic structure of the phosphonitrilic trimer–role of d orbitals in chemical bonding. Int J Quantum Chem 34:207–218. https://doi.org/10.1002/qua.560340824

[55.] Craig DP, Paddock NL (1962) 801.Electron distribution in cyclic pπ–dπ systems. J Chem Soc. https://doi.org/10.1039/JR9620004118

[56] Craig DP, Mitchell KAR (1965) 871."Island" and cyclic delocalisation in pπ–dπ systems. J Chem Soc. https://doi.org/10.1039/JR9650004682

[57] Paddock NL (1964) Phosphonitrilic derivatives and related compounds. Q Rev Chem Soc 18:168–210. https://doi.org/10.1039/QR9641800168

[58] Hadji D, Champagne B (2019) First principles investigation of the polarizability and first hyperpolarizability of anhydride derivatives. Chemistry Africa 2:443–453. https://doi.org/10.1007/s42250-019-00060-3

[59] Hadji D, Rahmouni A, Hammoutène D, Zekri O (2019) First theoretical study of linear and nonlinear optical properties of diphenyl ferrocenyl butene derivatives. J Mol Liq 286:110939. https://doi.org/10.1016/j.molliq.2019.110939

[60] Boukabene M, Brahim H, Hadji D, Guendouzi A (2020) Theoretical study of geometric, optical, nonlinear optical, UV–Vis spectra and phosphorescence properties of iridium(III) complexes based on 5–nitro–2–(2′,4′–difluorophenyl)pyridyl. Theor Chem Acc 139:47. https://doi.org/10.1007/s00214-020-2560-9

[61] Baroudi B, Argoub K, Hadji D, Benkouider AM, Toubal K, Yahiaoui A, Djafri A (2020) Synthesis and DFT calculations of linear and nonlinear optical responses of novel 2–thioxo–3–N, (4–methylphenyl) thiazolidine–4 one. J Sulfur Chem 41:1–16. https://doi.org/10.1080/17415993.2020.1736073

[62] Sim F, Chin S, Dupuis M, Rice J (1993) Electron correlation effects in hyperpolarizabilities of p–nitroaniline. J Phys Chem 97:1158–1163. https://doi.org/10.1021/j100108a010

[63] Pecul M, Pawłowski F, Jørgensen P, Köhn A, Hättig C (2006) High–order correlation effects on dynamic hyperpolarizabilities and their geometric derivatives: a comparison with density functional results. J Chem Phys 124:114101. https://doi.org/10.1063/1.2173253

[64] Zalesny R, Bartkowiak W, Toman P, Leszczynski J (2007) Computational insight into relations between electronic and vibrational polarizabilities within the two–state valence–bond charge–transfer model. J Chem Phys 337:77–80. https://doi.org/10.1016/j.chemphys.2007.06.031

[65] Zalesny R, Wójcik G, Mossakowska I, Bartkowiak W, Avramopoulos A, Papadopoulos MG (2009) Static electronic and vibrational first hyperpolarizability of meta–dinitrobenzene as studied by quantum chemical calculations. J Mol Struct (Theochem) 907:46–50. https://doi.org/10.1016/j.theochem.2009.04.011

[66] Andrea A (2013) Nonlinear optical properties of fluorobenzenes: a time-dependent hartree–fock study. Comput Theor Chem 1013:23–24. https://doi.org/10.1016/j.comptc.2013.03.014

[67] Choi JJ, Kim KM, Lim JS, Lee C, Kim DW (2007) Synthesis and characterization of dendritic nonlinear optical chromophore containing phenylene attached with bulky alkyl group. Macromol Res 15:59–64. https://doi.org/10.1007/BF03218753

[68] Pan Y, Tang X (2008) Synthesis and properties of novel Y–shaped nonlinear optical polymers containing imidazole–based chromophores. J Appl Poly Sci 108:2802–2807. https://doi.org/10.1002/app.27579

[69] Li Z, Qin J, Li S, Ye C, Luo J, Cao Y (2002) Polyphophazene Containing indole-based dual chromophores: synthesis and nonlinear optical characterization. Macromolecules 35:9232–9235. https://doi.org/10.1021/ma020769r

[70] Zoghaib WM, Husband J, Soliman UA, Shaaban IA, Mohamed TA (2013) Analysis of UV and vibrational spectra (FT-IR and FT-Raman) of hexachlorocyclotriphosphazene based on normal coordinate analysis, MP2 and DFT calculations. Spectrochim Acta A Mol Biomol Spectrosc 105:446–455. https://doi.org/10.1016/j.saa.2012.11.071

[71] Basharat M, Abbas Y, Hadji D, Ali Z, Zhang S, Ma H, Wu Z, Liu W (2020) Amorphous covalent inorganic–organic hybrid frameworks (CIOFs) with an aggregation induced selective response to UV–Visible light and their DFT studies. J Mater Chem C 8:13612–13620. https://doi.org/10.1039/D0TC01535K

[72] Hadji D, Rahmouni A (2015) Theoretical study of nonlinear optical properties of some azoic dyes. Med J Chem. 4:185–192. https://doi.org/10.13171/mjc.4.4.2015.15.07.22.50/hadji

[73] Hadji D, Brahim H (2018) Structural, optical and nonlinear optical properties and TD DFT analysis of heteroleptic bis cyclometalated iridium(III) complex containing 2 phenylpyridine and picolinate ligands. Theo Chem Acc 137:180. https://doi.org/10.1007/s00214-018-2396-8

[74] Bensafi T, Hadji D, Yahiaoui A, Argoub K, Hachemaoui A, Kenane A, Baroudi B, Toubal K, Djafri A, Benkouider AM (2021) Synthesis, characterization and DFT calculations of

linear and NLO properties of novel (Z)–5–benzylidene–3–N(4–methylphenyl)–2–thioxothiazolidin–4–one. J Sulf Chem 42:645–663. https://doi.org/10.1080/17415993.2021.1951729

[75] Benmohammed A, Hadji D, Guendouzi A, Mouchaal Y, Djafri A, Khelil A (2021) Synthesis, characterization, linear and NLO properties of novel N–(2,4–Dinitrobenzylidene)–3–Chlorobenzenamine schiff base: combined experimental and DFT calculations. J Elec Materi 50:5282–5293. https://doi.org/10.1007/s11664-021-09046-9

[76] Gheribi R, Hadji D, Ghallab R, Medjani M, Benslimane M, Trifa C, Dénès G, Merazig H (2021) Synthesis, spectroscopic characterization, crystal structure, Hirshfeld surface analysis, linear and NLO properties of new hybrid compound based on Tin fluoride oxalate and organic amine molecule $(C_{12}N_2H_9)_2[SnF_2(C_2O_4)_2]2H_2O$. J Mol Struct 1248:131392. https://doi.org/10.1016/j.molstruc.2021.131392

[77] Brandão I, Fonseca TL, Georg HC, Castro MA, Pontes RB (2020) Assessing the structure and first hyperpolarizability of $Li@B_{10}H_{14}$ in solution: a sequential QM/MM study using the ASEC–FEG method. Phys Chem Chem Phys 22:17314–17324. https://doi.org/10.1039/D0CP01268H

[78] Merouane A, Mostefai A, Hadji D, Rahmouni A, Bouchekara M, Ramdani A, Taleb S (2020) Theoretical insights into the static chemical reactivity and NLO properties of some conjugated carbonyl compounds: case of 5–aminopenta–2,4–dienal derivatives. Monatsh Chem 151:1095–1109. https://doi.org/10.1007/s00706-020-02653-y

[79] Bekki Y, Hadji D, Guendouzi A, Houari B, Elkeurti M (2021) Linear and nonlinear optical properties of anhydride derivatives: a theoretical investigation. Chem Data Collect 37:100809. https://doi.org/10.1016/j.cdc.2021.100809

[80] Muhammad S, AlSehemi AG, Irfan A, Chaudhry AR (2016) Tuning the push–pull configuration for efficient second–order nonlinear optical properties in some chalcone derivatives. J Mol Graph Model 68:95–105. https://doi.org/10.1016/j.jmgm.2016.06.0

[81] Muhammad S, Irfan A, Shkir M, Chaudhry AR, Kalam A, AlFaify S, AlSehemi AG, AlSalami AE, Yahia IS, Xu H-L, Su Z-M (2015) How does hybrid bridging core modification enhance the nonlinear optical properties in donor-π-acceptor configuration? a case study of dinitrophenol derivatives. J Comput Chem 36:118–128. https://doi.org/10.1002/jcc.23777